proceedings

MDPI

Proceedings

Toxic organic contaminants in airborne particles responsible for negative health effects

Donatella Pomata [1], Carmela Riccardi [1], Patrizia Di Filippo [1], Elisa Sonego [2], Giulia Simonetti [2,*], Federica Castellani [2] and Francesca Buiarelli [2]

[1] DIT, INAIL, Via Roberto Ferruzzi 38, 00143 Rome, Italy; d.pomata@inail.it, ca.riccardi@inail.it, p.difilippo@inail.it
[2] Department of Chemistry, Sapienza University of Rome, 00185 Rome, Italy; elisa.sonego@uniroma1.it, federica.castellani@uniroma1.it, francesca.buiarelli@uniroma1.it
* Correspondence: giulia.simonetti@uniroma1.it; Tel.: (+39)06 4991 3810

Abstract: Several studies indicate a strong correlation between airborne particulate matter (PM) and adverse health outcomes, as a function of particle size. Traditionally, the study of PM has focused on particles less than 10 or 2.5 μm in aerodynamic diameter (Da); however, recent evidence links particles less than 0.1 μm in Da and cardiovascular disease. In this study, we monitored 66 organic contaminants in size-fractionated PM samples collected in outdoor environments. The data obtained were analyzed with Principal Component Analysis (PCA), which showed a correlation between sites and classes of pollutants, allowing the identification of characteristic emission sources of each monitored site.

Keywords: Organic pollutant measurements; dimensional distribution profile; outdoor environments; Principal Component Analysis

1. Introduction

Particulate matter regional deposition in human respiratory tract is primarily based on the particle aerodynamic size [1]. In particular, ultrafine particles (UFs, less than 0.1 μm in aerodynamic diameter) may penetrate blood circulation, reach the inner organs [2-3], and distribute the toxic substances adsorbed on their surface. UFs have a greater surface area to mass ratio compared to larger particles, providing a larger area to adsorb potentially toxic chemicals [4]. Both the size and the composition of the airborne particles are closely related to the sources. In this optic, the study of ultrafine, fine, and coarse trace organic compositions can enhance the identification of different emission sources, characteristic of specific environments, and provide important insight into their contribution to adverse human health effects. Receptor models, applied to organic chemicals extracted from particles of different size collected in specific areas, can contribute to the identification of possible characteristic sources [5]. Among the receptor models, chemical mass balance, [6] positive matrix factorization [7] and principal component analysis (PCA) [5-8] are widely used to obtain source apportionment results. The aim of the present study was to identify characteristic or common emission sources in three workplaces and in an urban outdoor area. We applied the PCA to a data set, including 66 organic contaminant concentrations, analyzed in coarse (C), fine (F) and ultrafine (UF) particles, collected in the three workplaces and in the urban outdoor area. The concentrations were reported in ng per mg of PM sampled. The compounds analyzed belonged to six different groups of organic contaminants: polycyclic aromatic hydrocarbons (PAHs) and their derivatives (nitro-PAHs and oxy-PAHs), polychlorinated biphenyls (PCBs), polybrominated diphenyl ethers (PBDEs) and Novel Brominated flame-retardants (N-BFRs), selected for their toxicity and persistence in the environment.

2. Materials and Methods

2.1. Sampling

PM at different sizes was collected in four areas located in central Italy, in the same period of autumn 2017, to prevent weather conditions from affecting distribution of PM in outdoor atmospheres [9]. Particle collection was performed: in an outdoor urban area (RM); in an outdoor wastewater treatment plant (WWTP), during different phases of the process; in two different sites within an intensive livestock farming activity, nearby a shed used as stable (COW) and close to a shed for the grinding, mixing, and storing of feeds (FEED).

DLPI samplers (Dekati Low Pressure Impactor, Dekati, Kangasala, Finland), consisting of thirteen stages (from 10000 to 30 nm of aerodynamic diameter, Dp), operating at a flow rate of 10 L min^{-1}, were used to trap particles on Polycarbonate Membrane Filters, 0.45 μm pore size, 25 mm diameter (Merck Millipore, Merck S.p.a., Vimodrone, Milan, Italy). Before and after the samplings, pre-conditioned filters (50% R.H. and 20 °C) were weighed in triplicate to within ±0.001 mg, on a microbalance MC5 Sartorius, (Sartorius Lab Holding GmbH, Goettingen, Germany). After, the thirteen filters from each sampler were reassembled into three sets: an ultrafine fraction with $0.016<Da<0.094$ μm ($UF=PM_{0.1}$), a fine fraction with $0.15<Da<2.46$ μm ($F=PM_{0.1-2.5}$) and a coarse fraction corresponding to $3.63<Da<10$ μm ($C=PM_{2.5-10}$).

2.2. Analytical Methods

The analytical procedure was extensively described in a previous paper [10]. Briefly, filters were extracted by an accelerated solvent extractor ASE 200 (Dionex Sunnyvale, CA, USA) with DCM/n-Hexane (1:1) (two cycles) followed by ethyl acetate (two cycles) at 100°C and 1500 psi. The extracts were evaporated and re-dissolved with 50 μL of toluene until analytical determinations.

The analysis of PCBs, BDEs, NBFRs, PAHs, and PAH derivatives (oxy-PAHs and nitro-PAHs) were performed by gaschromatography-mass spectrometry (GC-MS). An HP 7890-B gas chromatograph fitted with an HP 7693 autosampler and coupled with an HP 5977B single quadrupole mass-selective detector (Agilent Technologies, Palo Alto, CA) was used for GC-MS analysis both in electronic ionization and in negative chemical ionization. Selective ion monitoring was used in both MS configurations. The injector temperature was set at 280 °C and the samples (1 μL) were injected in splitless mode. The helium carrier gas was set at a constant flow rate of 1.0 mL/min. Analytical methods were described in detail in previous studies [10-14].

3. Results and discussion

3.1. Organic compound concentrations

The method of standard addition, to minimize matrix effects, was used for the quantitative analysis of the 66 organic compounds. Each of the three extracts from ultrafine, fine and coarse particles were split in five aliquots and added with multistandard solutions of all analytes at growing concentrations. The absolute value of the x-intercept corresponded to the unknown concentration of the analyte. The concentrations of compounds belonging to the same group were added up to have one result for each class of organic species in each of the three fractions. Figure 1 shows the distribution of all groups of organic substances in the three fractions of PM in each of the four sampling site. All classes of compounds have a higher concentration per unit of PM at the FEED site in all the three particulate fractions; as regards UF, F and C fractions, the distribution of organic substances is proportional, but the finer is the fraction, the more concentrated are the organic substances, as can be seen by the different y-axis scales [15]. As expected, PAHs and derivatives contribute more significantly to the organic composition of particles, than other classes of compounds, due to a higher number of emission sources [16]. In particular, photochemical production is the source of the majority of nitro- and oxy- PAHs, as evidenced by the higher concentrations of those compounds produced in the atmosphere as secondary pollutants: 9- 2- and 3- nitro- phenanthrenes and 9-fluorenone in all the PM fractions (data not shown).

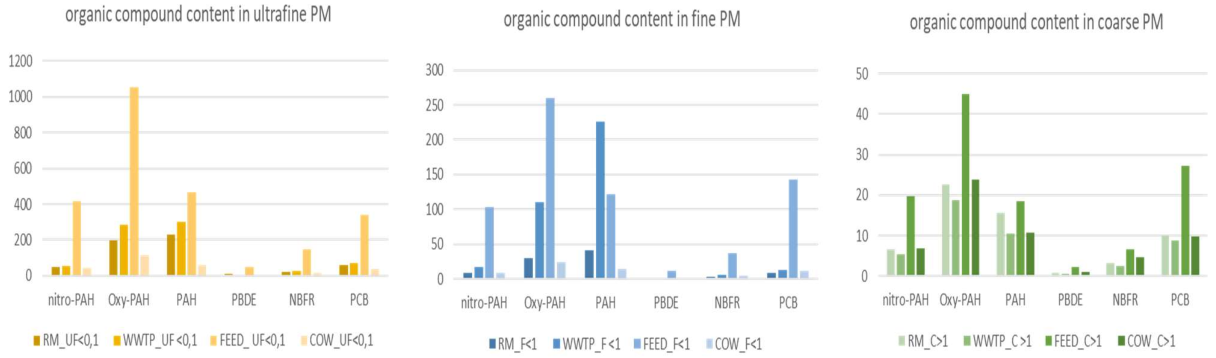

Figure 1. Distribution (ng per mg of PM) of all groups of organic substances in ultrafine, fine and coarse fractions of PM.

3.2. Principal component analysis (PCA)

Multivariate statistical computations were performed using the statistical software R (R-project for statistical computing, Ver. 3.0, 32-bit). A principal component analysis (PCA) was calculated on the matrix of data of figure 1, including the chemical concentrations (ng per mg of PM) of 14 PAHs, 9 Ox-PAHs, 10 Nitro-PAHs, 15 PCB, 7 PBDE and 11 NBFR, in the three PM dimensional fractions (UF<1, F>1 and C<10 μm), in the four different sampling sites. The data matrix was transformed by performing row and column autoscaling to overcome the scale variations between the examined variables [17]. Two principal component analyses were run on all compounds, and on the individual classes of contaminants (PAHs and derivatives, PCBs, PBDEs and NBFRs).

In Appendix A, Table A1 lists compounds and site codes used in PCA development.

3.2.1. All organic compounds

Figure 2 shows the loading plot and the score plot for all target compounds in all sampling sites and in the three PM dimensional fractions.

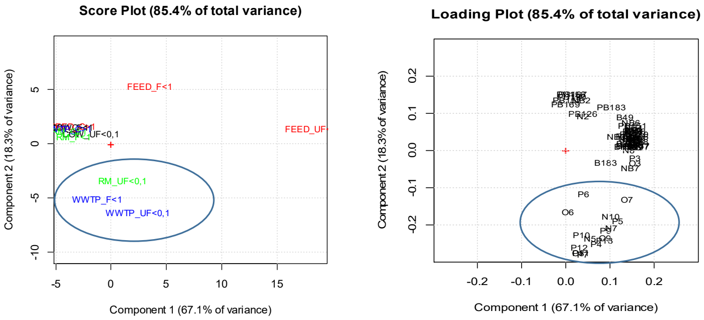

Figure 2. Loading plot and the score plot for all target compounds in all sampling sites and in the three PM dimensional fractions.

The two main components PC1 and PC2 explain 85.4% of total variance.

The score plot highlights a well-defined cluster, including WWTP F<1 and UF<0.1 and RM UF<0.1, that shows a significant correlation with the group of compounds positioned at the bottom of the loading plot (blue circles). This area corresponds to data relating to some PAHs and derivatives characteristic of anthropogenic sources. Furthermore, FEED F<1 and UF<0.1 also seem to be influenced by specific contamination sources, even if different from those identified in WWTP and RM sites. However, it is not possible to find any correlation with specific compounds as, in the upper part of the loading plot, the compounds are unevenly distributed and no cluster is shown.

More information can be obtained by considering the PCA carried out on each of the three macro-classes of compounds (PAHs and derivatives, PCBs, PBDEs and NBFRs).

3.2.2. Individual classes of organic compounds

Figure 3 shows loading and score plots for each single class of compounds.

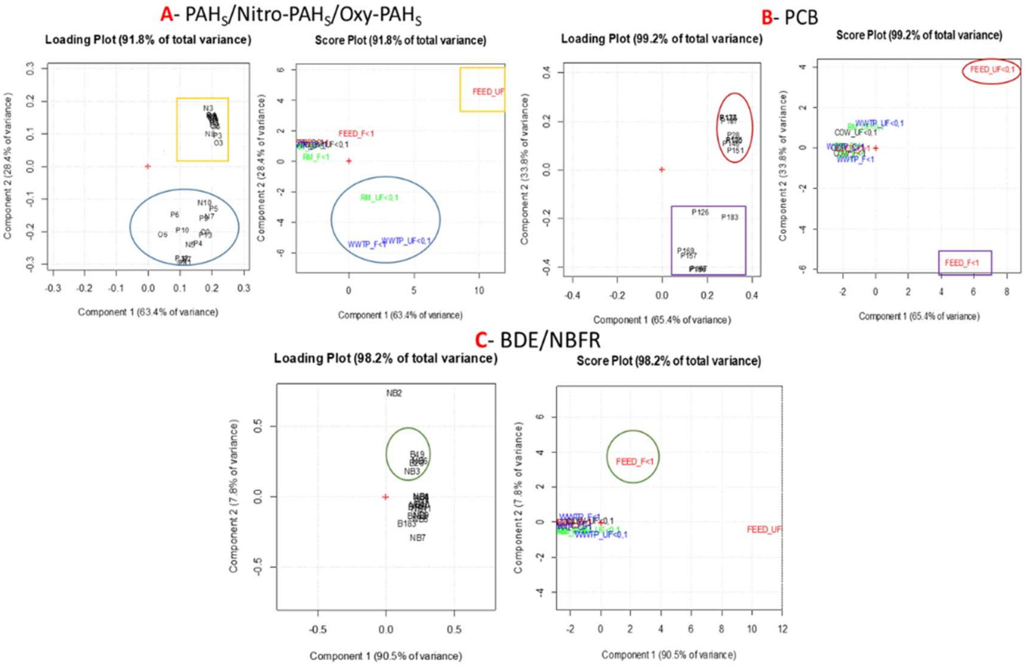

Figure 3. Loading and score plots of PCA carried out on the three classes of compounds: PAHs and derivatives (A), PCBs (B), PBDE and NBFR (C).

Plots relating to PAHs and derivatives (figure 3A) highlight a significant correlation among WWTP F<1, UF<0.1, RM UF<0.1 and the high molecular weight PAHs (HMW-PAHs), some NO- and Oxy-PAHs (blue circles). As HMWPAHs have a pyrolytic origin, this result suggests combustion as main source of contamination in WWTP and RM. The NO-PAHs that most affect the sites are 7NBaA and 9NA, both of primary origin and due to direct emissions from combustion processes, and 2NF of secondary origin by photochemical mechanisms. The good correlation with 9,10-Phenanthrenequinone, 1,9-Benz-10-anthrone and BaA-7,12-dione, generated by both combustion processes and reactions in atmosphere, further supports the hypothesis of combustion as predominant source of pollution for WWTP and RM in the fine and ultrafine fractions of PM [12-13]. Lastly, the PCA, carried out with PAH and derivative data, also highlights that WWTP and RM sites are influenced by similar emission sources in agreement with their location.

PCBs show a good correlation with feed site for fine and ultrafine PM fraction (Figure 3B). FEED F<1 correlates with 5 dioxin-like PCBs (126, 156, 157, 167 and 169) (purple square), while FEED UF<0.1 is influenced by others PCBs including also PCB28 and 138 (red circles). These two compounds, with PCB52, 101, 153 and 180 are considered indicators of contamination in food and feed and their sum includes about half of the total amount of no dioxin-like PCBs detected in these matrices [18]. WWTP and RM sites do not seem to be influenced by PCB sources.

PBDE and NBFR classes show a significant correlation with feed site for fine PM fraction (figure 3C). A well-defined cluster is highlighted in the upper part of the loading plot (green circles) related to the FEED<1. The compounds which characterize this group are BDE28 and 49, PBEBs and TBPs in agreement with Fernandes et al. [19] that have detected the presence of PBDEs and some NBFRs in animal feed at non-negligible concentrations. As well as for PCBs, WWTP and RM sites do not show any correlation with PBDE and NBFR.

4. Conclusions

Because epidemiological studies mainly link the carcinogenic effects of exposure to UF, F and coarse PM emissions to the organic fraction, samplings and organic speciation for the three fractions of aerosols in three working environments and in an urban one were investigated and submitted to principal component analysis. In this study, the results obtained showed that the finer is the PM fraction, the more concentrated are the organic substances. From PCA analysis, specific correlations between the two sites WWTP and RM show WWTP mainly affected by urban sources. On the contrary, FEED site seems to be influenced by specific contamination sources, different from those identified in all the other sites, causing extremely high concentrations of organic contaminants.

Author Contributions: Donatella Pomata (D.P.), Carmela Riccardi (C.R.), Patrizia Di Filippo (P.DF.), Elisa Sonego (E.S.), Giulia Simonetti (G.S.) Federica Castellani (F.C.) and Francesca Buiarelli (F.B.) "Conceptualization, C.R. and G.S.; methodology, F.C.; software, G.S.; validation, C.R.; formal analysis, E.S. and D.P; investigation, F.B.; resources, F.B.; data curation, P.DF. and D.P; writing—original draft preparation, G.S.; writing—review and editing, C.R.; visualization, P.DF.; supervision, F.B.; project administration, C.R.; funding acquisition, F.B.

Funding: "This research was funded by INAIL Ricerca Scientifica 2019-2021

Conflicts of Interest: "The authors declare no conflict of interest." "The funders had no role in the design of the study; in the collection, analyses, or interpretation of data; in the writing of the manuscript, or in the decision to publish the results".

Appendix A

Table A1. Organic compound list and codes used in PCA development.

PAHs	PCA code	Oxy-PAHs	PCA code	Nitro-PAHs	PCA code
Anthracene	P1	9-Fluorenone	O1	2-N-Fluorene	N1
Fluoranthene	P2	1,8-Naphthalic anhydride	O2	2-N-Anthracene	N2
Pyrene	P3	4H-Cyclopenta[def]phenanthrene-4-one	O3	2-N-Phenanthrene	N3
Benz[a]anthracene	P4	1,4-Phenanthrenedione	O4	3-N- Phenanthrene	N4
Chrysene +Trif	P5	9,10-Anthracene-dione	O5	9-N- Anthracene	N5
Benz[k]fluoranthene	P6	9,10-Phenanthrenequinone	O6	9-N- Phenanthrene	N6
Benz[b]fluoranthene	P7	Benz[a]fluorenone	O7	2-N-Fluoranthene	N7
Benz[a]fluoranthene	P8	1,9-Benz-10-anthrone	O8	1-N-Pyrene	N8
Benz[e]pyrene	P9	Benzo[a]anthracene-7,12-dione	O9	3-N-Fluoranthene	N9
Benz[a]pyrene	P10			7-N-benz[a]anthracene	N10

Benz[ghi]perylene	P11				
Indeno[1,2,3-cd]pyrene	P12				
Coronene	P13				
PCBs	**PCA code**	2,2',3,3',4',5,6-Heptachlorobiphenyl	PB177	**NBFRs**	**PCA code**
2,4,4′-Trichlorobiphenyl	PB28	2,2',3,4,4',5',6-Heptachlorobiphenyl	PB183	2,4-Dibromophenol	NB1
2,3,3′,4,4′-Pentachlorobiphenyl	PB105	2,2',3,4',5,5',6-Heptachlorobiphenyl	PB187	2,6-Dibromophenol	NB2
3,3',4',4',5 Pentachlorobiphenyl	PB126	2,3,3',4,4',5,6-Heptachlorobiphenyl	PB190	2,4,6-Tribromophenol	NB3
2,2′,3,4,4′,5′-Hexachlorobiphenyl	PB138	**PBDEs**	**PCA code**	Allyl-2,4,6-tribromophenyl ether	NB4
2,2',3,4',5,5'-Hexachlorobiphenyl	PB146	2,4,4'-Tribromodiphenyl ether	B28	1,2-dibromo-4-(1,2-dibromoethyl) cyclohexane	NB5
2,2′,3,5,5′,6-Hexachlorobiphenyl	PB151	2,2',4,4'-Tetrabromodiphenyl ether	B47	2,3,4,5,6-pentabromoethylbenzene	NB6
2,3,3′,4,4′,5-Hexachlorobiphenyl	PB156	2,2',4,5'-Tetrabromodiphenyl ether	B49	2,3-dibromopropyl-2, 4, 6-tribromophenylether	NB7
2,3,3',4,4',5'-Hexachlorobiphenyl	PB157	2,2′,4,4′,5-Pentabromodiphenyl ether	B99	Hexabromobenzene	NB8
2,3',4,4',5,5'-Hexachlorobiphenyl	PB167	2,2′,4,4′,6-Pentabromodiphenyl ether	B100	2-Ethylhexyl-2,3,4,5-tetrabrombenzoate	NB9
3,3',4,4',5,5'-Hexachlorobiphenyl	PB169	2,2',4,4',5,5'-Hexabromodiphenyl ether	B153	1,2-bis(2,4,6-tribromophenoxy) ethane	NB10
2,2′,3,3′,4,4′,5-Heptachlorobiphenyl	PB170	2,2',3,4,4',5',6-Heptabromodiphenyl ether	B183	bis (2-ethylhexyl)-3,4,5,6-tetrabromophthalate	NB11

References

1. Carvalho, T.C.; Jay, I.P., Robert O.W.III. Influence of particle size on regional lung deposition – What evidence is there? *Int. J. Pharm.* **2011**, *406*, 1–10.
2. Knol, A.B., de Hartog, J.J., Boogaard, H., Slottje, P., van der Sluijs, J.P., Lebret, E., Brunekreef, B. Expert elicitation on ultrafine particles: likelihood of health effects and causal pathways. *Part Fibre Toxicol* **2009**, 6(1), 19.
3. Wichmann, H. E., Peters, A. Epidemiological evidence of the effects of ultrafine particle exposure. In *Ultrafine particles in the atmosphere* **2000**, 243-267.
4. Oberdörster, G. Pulmonary effects of inhaled ultrafine particles. *Int Arch Occup Environ Health* **2000**, *74*(1), 1-8.
5. Belis, C.A., Karagulian, F., Larsen, B.R., Hopke, P.K. Critical review and meta-analysis of ambient particulate matter source apportionment using receptor models in Europe. *Atmos Environ* **2013**, *69*, 94–108
6. Shi, G.L., Zeng, F., Li, X., Feng, Y.C., Wang, Y.Q., Liu, G.X., Zhu, T. Estimated contributions and uncertainties of PCA/MLR-CMB results: source apportionment for synthetic and ambient datasets. *Atmos Environ* **2011**, *45*, 2811–2819
7. Manousakas, M., Papaefthymiou, H., Diapouli, E., Migliori, A., Karydas, A. G., Bogdanovic-Radovic, I., & Eleftheriadis, K. Assessment of PM2.5 sources and their corresponding level of uncertainty in a coastal urban area using EPA PMF 5.0 enhanced diagnostics. *Sci Total Environ* **2017**, *574*, 155-164.
8. Diapouli, E., Manousakas, M., Vratolis, S., Vasilatou, V., Maggos, T., Saraga, D., Th Grigoratosb, G. Argyropoulosb, D. Voutsab, C. Samarab, K. & Eleftheriadis, K. Evolution of air pollution source contributions over one decade, derived by PM$_{10}$ and PM$_{2.5}$ source apportionment in two metropolitan urban areas in Greece. *Atmos Environ* **2017**, *164*, 416-430.
9. D'Innocenzio, F., Di Filippo, P., Lepore, L., Marconi, A. PM10 and PM2.5 concentrations in urban air and size fraction distribution of toxic metals. *Ann Chim* **1998**, 88(3-4), 281-289
10. Pomata, D., Di Filippo, P., Riccardi, C., Rossi, V., Simonetti, G., Sonego, E., & Buiarelli, F. Method optimisation for the simultaneous determination of legacy and emerging halogenated flame retardants in particulate matter collected in an electronic waste recycling facility. *Int J Environ Anal Chem* **2020**, *100*(13), 1479-1496.

11. Buiarelli, F.; Di Filippo, P.; Pomata, D.; Riccardi, C.; Bartocci, M. A liquid chromatography tandem mass spectrometry method for simultaneous analysis of 46 atmospheric particulate-phase persistent organic pollutants and comparison with gas chromatography/mass spectrometry. *Int J Environ Ana Chem* **2017**, *97*, 797–818.
12. Di Filippo, P.; Pomata, D.; Riccardi, C.; Buiarelli, F.; Gallo, V. Oxygenated polycyclic aromatic hydrocarbons in size-segregated urban aerosol. *J Aerosol Sci* **2015**, *87*, 126–134
13. Di Filippo, P., Riccardi, C., Pomata, D., & Buiarelli, F. Concentrations of PAHs, and nitro-and methyl-derivatives associated with a size-segregated urban aerosol. *Atmos Environ* **2010**, *44*(23), 2742-2749.
14. Borsella, E., Di Filippo, P., Riccardi, C., Spicaglia, S., & Cecinato, A. Data quality of PAH determinations in environmental monitoring. *Ann. Chim* **2004**, 94(9-10), 691-698.
15. Di Filippo, P., Riccardi, C., Incoronato, F., Sallusti, F., Spicaglia, S., & Cecinato, A. Characterization of selected speciated organic compounds associated with particulate matter in ambient air of the outskirts of Rome. *Polycycl Aromat Compd* **2005**, *25*(5), 393-406.
16. Cecinato, A.; Mabilia, R.; Brachetti, A.; Di Filippo, P.; Liberti, A. Nitrated-PAH in urban air of Italy as indicators of motor vehicle emission and light-induced reactions. *Anal Lett* **2001**, *34*, 927–936.
17. Bro, R., & Smilde, A. K. Centering and scaling in component analysis. *J Chemom* **2003**, *17*(1), 16-33.
18. European Commission. Commission Regulation (EU) No 1259/2011 of 2 December 2011 amending Regulation (EC) No 1881/2006 as regards maximum levels for dioxins, dioxin-like PCBs and non dioxin-like PCBs in foodstuffs. *Off J Eur Union*, **2011**,*320*, 18-23.
19. Fernandes, A. R., Mortimer, D., Rose, M., Smith, F., Panton, S., & Garcia-Lopez, M. Bromine content and brominated flame retardants in food and animal feed from the UK. *Chemosphere* **2016**, *150*, 472-478.